

Photon rest mass from localized fast radio bursts with improved distribution of dispersion measure from extragalactic gas

Yuchen Zhang^{},¹ Yang Liu^{},² Hongwei Yu^{},^{1,*} and Puxun Wu^{},^{1,†}

¹*Department of Physics, Hunan Research Center of the Basic Discipline for Quantum Effects and Quantum Technologies, and Key Laboratory of Low-Dimensional Quantum Structures and Quantum Control of Ministry of Education, Hunan Normal University, Changsha, Hunan 410081, China*

²*Purple Mountain Observatory, Chinese Academy of Sciences, No. 10 Yuanhua Road, Nanjing 210023, China*

arXiv:2511.14163v2 [astro-ph.CO] 23 Jan 2026

Abstract

The assumption that photons are massless is a foundational postulate of modern physics, yet it remains subject to experimental verification. Fast radio bursts (FRBs), with their cosmological distances and precisely measured dispersion, offer an excellent laboratory for testing this hypothesis. In this work, we propose an improved distribution function for the dispersion measure arising from extragalactic gas and demonstrate that it provides an excellent fit to mock data. We then apply this distribution to constrain the photon rest mass under the Λ CDM, w CDM, and w_0w_a CDM cosmological models, the last of which is favored by recent DESI baryon acoustic oscillation observations. The corresponding 1σ upper limits on the photon mass are found to be 4.83×10^{-51} kg, 4.71×10^{-51} kg, and 4.86×10^{-51} kg, respectively, which are the most stringent constraints derived from FRBs to date. These results demonstrate that FRBs provide robust and reliable constraints, and offer strong empirical support for the massless nature of the photon.

I. INTRODUCTION

A central postulate of Einstein's special relativity is the invariance of the speed of electromagnetic waves [1]: the speed of light in vacuum is constant, independent of the motion of either the source or the observer. This principle implies that photons must have zero rest mass since a non-zero photon mass would result in a frequency-dependent group velocity of photons, causing higher-frequency components to travel faster than the lower-frequency ones. Consequently, photons emitted simultaneously from the same source will exhibit a frequency-dependent time delay upon arrival, providing an opportunity to experimentally test whether photons are massless.

Numerous ground tests have been conducted to measure variations in the speed of light in order to examine the photon rest mass [2–6]. In recent years, astrophysical observations, especially gamma-ray bursts, have emerged as powerful probes for the relative propagation speeds of electromagnetic signals over cosmological distances [7–13]. Because light from distant sources travels for billions of years, even minuscule variations in photon speed can accumulate into measurable time delays, enabling exceptionally stringent constraints on a

* hwyu@hunnu.edu.cn

† pxwu@hunnu.edu.cn

possible photon mass.

Fast radio bursts (FRBs), enigmatic radio transients discovered in recent decades [14], are generally accepted to have a cosmic origin. Given that residual baryons are believed to exist in diffused state in the intergalactic medium (IGM), the ionized electrons arising from these baryons interact with the radio signals, leading to a time delay in their arrival. This delay is quantified by the dispersion measure (DM). There have already been numerous applications of the dispersion measures (DMs) of localized fast radio bursts (FRBs) to explore the cosmic reionization history [15–20] and constrain cosmological parameters, such as the Hubble constant H_0 [21–27], the present cosmic baryon density parameter Ω_{b0} and the baryon fraction in the diffused state (i.e. f_d) [28–42], and so on. When we assume a non-zero rest mass for the photon, the DM will include an additional contribution from the mass term, thereby creating a promising tool to constrain the photon rest mass using FRBs [43–54].

A key ingredient in FRB cosmology is the distribution function of the extragalactic DM, DM_{cosmic} , which accounts for contributions from the IGM and intervening halos. A widely used DM_{cosmic} distribution was proposed based on semi-analytic models and hydrodynamic simulations [38, 55], with fixed parameters $\alpha = \beta = 3$. Recently, Konietzka et al. [56] introduced a new method for measuring DM_{cosmic} in the IllustrisTNG cosmic simulation. They found that previous work [55] had misestimated the standard deviation and higher moments of the DM_{cosmic} distribution by over 50%. They constructed an analogue distribution of DM_{cosmic} similar to that in [38] and confirmed that this distribution, with parameters $\alpha \approx 1$ and $\beta \approx 3.3$, provides good fits across all redshifts. However, the distribution function presented in [56] does not explicitly contain information of our universe, and therefore cannot be used directly to estimate cosmological parameters.

In this paper, we first construct an improved distribution function of DM_{cosmic} that incorporates cosmological information, allowing the parameters α and β to vary with redshift. We find that our function is more consistent with mock data compared to those proposed in [38, 56].

We then utilize our distribution function to constrain the photon rest mass using FRB observations. Since FRBs are predominantly emitted from extragalactic sources, it is essential to select a specific cosmological model. The Λ CDM model, which consists of cosmological constant Λ and cold dark matter, is typically employed in such analyses [48–54, 57–59].

However, recent baryon acoustic oscillation (BAO) measurements from the Dark Energy Spectroscopic Instrument (DESI) Data Release 2 (DR2) indicate a strong preference for dynamical dark energy over the cosmological constant dark energy with a confidence level (CL) exceeding 3σ [60]. This motivates us to reanalyze photon mass constraints within cosmological models accommodating dynamical dark energy, such as the w CDM and w_0w_a CDM models [61, 62]. To constrain the parameters of these cosmological models, we combine data from Pantheon+ type Ia supernovae (SN Ia) [63], BAO from DESI [60], and the cosmic microwave background (CMB) from Planck [64].

This paper is organized as follows. In Sec. II, we provide a detailed description of the effective DM arising from a non-zero photon mass. In Sec. III, we present the observational datasets used, including FRB, CMB, BAO, and SN data. Our cosmological constraints are reported in Sec. IV. Finally, we summarize our conclusions and discussions in Sec. V.

II. DM FROM PHOTON MASS

If photons possess a non-zero rest mass m_γ , the energy of a single photon is

$$E = \sqrt{p^2c^2 + m_\gamma^2c^4}, \quad (1)$$

where p is the photon momentum and c is the speed of light. From Eq. (1), the corresponding group velocity of a photon with frequency ν becomes

$$v = \frac{\partial E}{\partial p} = c\sqrt{1 - \frac{m_\gamma^2c^4}{h_p^2\nu^2}} \approx c\left(1 - \frac{1}{2}A\nu^{-2}\right), \quad (2)$$

where $A \equiv \frac{m_\gamma^2c^4}{h_p^2}$ and h_p is the Planck constant. The approximation is valid only for a very small photon mass, $m_\gamma \ll E/c^2 \approx 7 \times 10^{-42} \left(\frac{\nu}{\text{GHz}}\right) \text{ kg}$ [50]. Eq. (2) indicates that if $m_\gamma \neq 0$, the speed of light becomes frequency-dependent, with higher-frequency photons propagating faster.

We now consider an astrophysical source at redshift z emitting radiation with high and low frequencies ν_h and ν_l . If the high-frequency photons arrive at $z = 0$, the low-frequency photons, traveling more slowly, arrive at time $-\Delta z$ (with $\Delta z \ll 1$). The comoving distances traveled by the two components are

$$x_{\nu_h} = \frac{c}{H_0} \int_0^z \left[1 - \frac{1}{2}A\nu_h^{-2}(1+z')^{-2}\right] \frac{dz'}{\tilde{E}(z')}$$

and

$$x_{\nu_l} = \frac{c}{H_0} \int_{-\Delta z}^z \left[1 - \frac{1}{2} A \nu_l^{-2} (1+z')^{-2} \right] \frac{dz'}{\tilde{E}(z')},$$

where H_0 is the Hubble constant, $\tilde{E}(z) = H(z)/H_0$ is the dimensionless Hubble parameter. The factor $(1+z)^{-2}$ accounts for cosmic redshift of the photon frequency. Since both photon components originate from the same source, their comoving distances must be equal, i.e., $x_{\nu_h} = x_{\nu_l}$, which leads to

$$\Delta z \simeq \frac{A}{2} (\nu_l^{-2} - \nu_h^{-2}) H_\gamma(z), \quad (3)$$

where

$$H_\gamma(z) \equiv \int_0^z \frac{(1+z')^{-2}}{\tilde{E}(z')} dz'. \quad (4)$$

The corresponding time delay induced by the photon mass is then

$$\Delta t_{m_\gamma} = \frac{\Delta z}{H_0} \simeq \frac{A}{2H_0} (\nu_l^{-2} - \nu_h^{-2}) H_\gamma(z). \quad (5)$$

The time delay due to $m_\gamma \neq 0$ can be interpreted as an effective DM [48–50, 59],

$$\text{DM}_\gamma = \Delta t_{m_\gamma} \frac{8\pi^2 m_e \epsilon_0 c}{e^2} (\nu_l^{-2} - \nu_h^{-2})^{-1} = \frac{4\pi^2 m_e \epsilon_0 c^5}{h_p^2 e^2} \frac{H_\gamma(z)}{H_0} m_\gamma^2. \quad (6)$$

Here ϵ_0 represents the permittivity of vacuum, e is the electron charge, and m_e is the mass of electron.

By comparing the observed DM with Eq. (6), we may constrain the photon rest mass. Since $H_\gamma(z)$ depends on the expansion history, adopting a cosmological model is essential. Motivated by recent DESI BAO results favoring dynamical dark energy, we consider three flat cosmological models, i.e., Λ CDM, w CDM and $w_0 w_a$ CDM. Their dimensionless Hubble parameters are

$$\tilde{E}(z) = \begin{cases} \sqrt{\Omega_{m0}(1+z)^3 + \Omega_{r0}(1+z)^4 + (1 - \Omega_{m0} - \Omega_{r0})} & \Lambda\text{CDM} \\ \sqrt{\Omega_{m0}(1+z)^3 + \Omega_{r0}(1+z)^4 + (1 - \Omega_{m0} - \Omega_{r0})(1+z)^{3(1+w)}} & w\text{CDM} \\ \sqrt{\Omega_{m0}(1+z)^3 + \Omega_{r0}(1+z)^4 + (1 - \Omega_{m0} - \Omega_{r0})(1+z)^{3(1+w_0+w_a)} e^{-3w_a \frac{z}{1+z}}} & w_0 w_a \text{CDM}. \end{cases} \quad (7)$$

Here Ω_{m0} and Ω_{r0} are the present matter and radiation density parameters, and w , w_0 and w_a are constants characterizing dynamical dark energy. The radiation density is given by

$$\Omega_{r0} = \Omega_{\gamma 0} (1 + 0.2271 N_{eff}), \quad (8)$$

where $\Omega_{\gamma 0} = \frac{3}{4h^2 \cdot 31500} \left(\frac{T_{\text{CMB}}}{2.7\text{K}}\right)^4$ is the present photon energy density with $h \equiv H_0/100 \text{ km s}^{-1} \text{ Mpc}^{-1}$ and $T_{\text{CMB}} = 2.7255 \text{ K}$ [65], and $N_{\text{eff}} = 3.044$ represents the effective number of relativistic species. To break degeneracies between cosmological parameters and the photon mass, we include complementary datasets: SN Ia, CMB and BAO.

III. OBSERVATIONAL DATA

A. FRB

For FRBs, the observed dispersion measure, DM_{obs} , contains contributions from several astrophysical sources as well as a potential contribution from a non-zero photon mass:

$$\begin{aligned} \text{DM}_{\text{obs}}(z) &= \text{DM}_{\text{astro}} + \text{DM}_{\gamma} \\ &= \text{DM}_{\text{ISM}}^{\text{MW}} + \text{DM}_{\text{halo}}^{\text{MW}} + \text{DM}_{\text{cosmic}}(z) + \text{DM}_{\text{host}}/(1+z) + \text{DM}_{\gamma}, \end{aligned} \quad (9)$$

where the superscript MW denotes the Milky Way, and the subscripts refer to contributions from the interstellar medium (ISM), the Milky Way halo, the cosmic baryon contribution (including the IGM and intervening halos [28]), the FRB host galaxy, and the photon-mass term.

Due to significant fluctuations in the distribution of baryons along the signal path, only the average cosmic dispersion measure $\langle \text{DM}_{\text{cosmic}} \rangle$ can be computed reliably. Its theoretical expression is [66, 67]:

$$\langle \text{DM}_{\text{cosmic}} \rangle = \frac{3c\Omega_{b0}H_0f_d}{8\pi Gm_p} \int_0^z \frac{(1+z')\chi_e(z')}{\tilde{E}(z')} dz' \quad (10)$$

where Ω_{b0} is the present cosmic baryon density fraction parameter, m_p is the photon mass, and f_d is the baryon mass fraction in the diffuse state. Following [40, 41], we treat f_d as a constant, despite the expectation of an increasing trend with redshift [68, 69]. For redshifts $z < 3$, hydrogen and helium are fully ionized, giving $\chi_e = 7/8$ [70, 71], which describes the number of free electrons per baryon. The Milky Way ISM contribution $\text{DM}_{\text{ISM}}^{\text{MW}}$ can be subtracted from the observed dispersion measure using electron-density models such as NE2001 and YMW16 [72, 73]. In this work, we adopt NE2001. For the Milky Way halo, Prochaska et al. [68] estimates $\text{DM}_{\text{halo}}^{\text{MW}}$ to lie between 50 and 80 pc cm^{-3} . Therefore, we impose a Gaussian prior $\mathcal{N}(65, 15^2)$ (pc cm^{-3}) truncated to this interval, though some recent studies suggest that $\text{DM}_{\text{halo}}^{\text{MW}}$ may take a lower value [74, 75].

Even after removing these Milky Way contributions, degeneracies remain among the cosmic, host, and photon-mass components. Following Macquart et al. [38], we define DM'_{ext} as DM corrected for contributions from the ISM and the halo:

$$\begin{aligned} DM'_{\text{ext}} &= DM_{\text{obs}} - DM_{\text{ISM}}^{\text{MW}} - DM_{\text{halo}}^{\text{MW}} \\ &= DM_{\text{cosmic}} + DM_{\text{host}}/(1+z) + DM_{\gamma} \equiv DM_{\text{ext}} + DM_{\gamma}, \end{aligned} \quad (11)$$

The probability distribution function (PDF) of DM_{ext} , including cosmic and host contributions, is

$$\begin{aligned} P(DM_{\text{ext}}) &= \int_0^{(DM'_{\text{ext}} - DM_{\gamma})(1+z)} \frac{1}{\langle DM_{\text{cosmic}} \rangle} P_{\text{host}}(DM_{\text{host}}) \\ &\times P_{\text{cosmic}} \left(\frac{DM'_{\text{ext}} - DM_{\text{host}}/(1+z) - DM_{\gamma}}{\langle DM_{\text{cosmic}} \rangle} \right) dDM_{\text{host}}. \end{aligned} \quad (12)$$

This expression originates from Macquart et al. [38], although they omitted the normalization factor $\frac{1}{\langle DM_{\text{cosmic}} \rangle}$ [76, 77]. Let $\Delta \equiv DM_{\text{cosmic}}/\langle DM_{\text{cosmic}} \rangle$, the cosmic-component PDF, $P_{\text{cosmic}}(\Delta)$, is found to satisfy

$$P_{\text{cosmic}}(\Delta) = A\Delta^{-\beta} \exp \left[-\frac{(\Delta^{-\alpha} - 1)^2}{2\alpha^2\sigma_{\text{cosmic}}^2} \right], \quad \Delta > 0, \quad (13)$$

where A is the normalization constant, and α , β and σ_{cosmic} are model parameters. This formula differs slightly from that proposed by Macquart et al. [38] (see Eq. (A1)) as we fix $C_0 = 1$. In [38], α and β were both set to 3 and $\sigma_{\text{cosmic}} = F \times z^{-0.5}$, with F being a free parameter. Based on the continuous DM_{cosmic} catalog, Konietzka et al. [56] found that the PDF of DM_{cosmic} takes a similar form to that of Eq. (13), with parameters $\alpha \approx 1$ and $\beta \approx 3.3$, which fits well with their simulation data. In our analysis, we treat α , β and σ_{cosmic} as free parameters and calibrate them with mock data. The Kolmogorov–Smirnov test indicates that allowing all three parameters to vary provides a significantly better description of DM_{cosmic} (see Appendix. A for details).

We model the host-galaxy DM, $P_{\text{host}}(DM_{\text{host}})$, as a log-normal distribution

$$P_{\text{host}}(DM_{\text{host}}) = \frac{1}{\sqrt{2\pi}DM_{\text{host}}\sigma_{\text{host}}} \times \exp \left[-\frac{(\ln DM_{\text{host}} - \mu_{\text{host}})^2}{2\sigma_{\text{host}}^2} \right]. \quad (14)$$

The parameters μ_{host} and σ_{host} are adopted from the IllustrisTNG simulations [78] within $0.1 < z < 1.5$,¹ and their values at each redshift are obtained via cubic-spline interpolation.

¹ Note that [78] presents the mean and standard deviation for $\ln(DM_{\text{host}}/(1+z))$, rather than for $\ln DM_{\text{host}}$.

It should be noted that the IllustrisTNG simulation in [78] is conducted within the framework of Λ CDM cosmology. Therefore, potential incompatibilities may arise when estimating parameters in other cosmological models. To investigate whether such incompatibilities affect the posterior constraints, we additionally treat μ_{host} and σ_{host} as free parameters, similar to what was done in [38, 79], and compare the corresponding results with those derived from the IllustrisTNG-based prescription.

From the FRB likelihood function, $\ln \mathcal{L}_{\text{FRB}} = \ln P(\text{DM}_{\text{ext}})$, we can derive constraints on the photon mass and cosmological parameters from FRBs. Recently, a collection of 115 localized FRBs was compiled in [80], with the highest redshift $z = 1.354$. This large dataset significantly enhances our ability to constrain free parameters. In this compilation, FRB190520B and FRB220831A are excluded due to their extremely high DM_{obs} , and FRB220319D is discarded because it has a negative DM_{ext} . Additionally, FRB20221027A is excluded for its ambiguity in the host galaxy localization [81]. Considering that DM_{halo} is restricted to $(50, 80) \text{ pc cm}^{-3}$, we impose the additional condition: $\text{DM}_{\text{obs}} - \text{DM}_{\text{ISM}}^{\text{MW}} > 80 \text{ pc cm}^{-3}$ as filters to ensure physical consistency. We also require $z > 0.02$, because the parameters in the PDF start at $z = 0.02$. After applying these cuts, 104 FRBs remain for our analysis.

B. SN Ia

The SN Ia data utilized in our analysis come from the Pantheon+ compilation, which consists of 1701 supernovae with redshifts in the range $z \in [0.00122, 2.26137]$ [63]. To reduce the impact of peculiar velocities on very nearby events [82], we discard all objects with redshift $z \leq 0.01$, leaving 1590 supernovae in our final sample. The distance module μ of SN Ia is defined as $\mu = m - M$, where m is the SN apparent magnitude and M is the absolute magnitude, treated as a nuisance parameter that is marginalized over in the analysis. The theoretical distance module for a SN Ia can be evaluated using the following formula:

$$\mu_{\text{th}} = 25 + 5 \log_{10} \left(\frac{D_{\text{L}}(z)}{\text{Mpc}} \right), \quad (15)$$

where D_{L} is the luminosity distance, calculated as $D_{\text{L}} = \frac{c(1+z)}{H_0} \int_0^z \frac{dz'}{E(z')}$ in a spatially flat universe. The log-likelihood function for SN Ia can be expressed in terms of the observed

distance modules and the corresponding model predictions:

$$\ln \mathcal{L}_{\text{SN}} \propto -\frac{1}{2}(\boldsymbol{\mu}_{\text{obs}} - \boldsymbol{\mu}_{\text{th}})^{\text{T}} \mathbf{C}_{\text{SN}}^{-1} (\boldsymbol{\mu}_{\text{obs}} - \boldsymbol{\mu}_{\text{th}}) \quad (16)$$

with \mathbf{C}_{SN} the covariance matrix of the observed distance moduli.

C. CMB

For CMB data, we use the Planck 2018 results [64]. Instead of the CMB temperature and polarization power spectra, we consider three derived parameters: the acoustic scale l_{A} , the shift parameter R and $\Omega_{b0}h^2$ from the Planck 2018 data [65] for simplifying numerical calculation. The theoretical expression of l_{A} is

$$l_{\text{A}}(z^*) = (1 + z^*) \frac{\pi D_{\text{A}}(z^*)}{r_{\text{s}}(z^*)}, \quad (17)$$

where $z^* = 1089.92$ [64] is the redshift at the photon decoupling epoch, $D_{\text{A}} = D_{\text{L}}/(1 + z)^2$ is the angular diameter distance, and r_{s} is the comoving sound horizon, defined as

$$r_{\text{s}}(z) = \frac{c}{H_0} \int_0^{1/(1+z)} \frac{da}{a^2 \tilde{E}(a) \sqrt{3 \left(1 + \frac{3\Omega_{b0}h^2}{4\Omega_{\gamma 0}h^2} a\right)}}. \quad (18)$$

Here $a = 1/(1 + z)$ is the scale factor. The shift parameter R takes the form

$$R(z^*) = (1 + z^*) \frac{D_{\text{A}}(z^*) \sqrt{\Omega_{m0}} H_0}{c}. \quad (19)$$

Introducing the vector $\mathbf{A}_{\text{CMB}} = \{R, l_{\text{A}}, \Omega_{b0}h^2\}$, the Planck CMB observations give $\mathbf{A}_{\text{CMB,obs}} = \{1.7502, 301.471, 0.02236\}$. Then we find that the expression of the log-likelihood function for the CMB data is

$$\ln \mathcal{L}_{\text{CMB}} \propto -\frac{1}{2}(\mathbf{A}_{\text{CMB,obs}} - \mathbf{A}_{\text{CMB,th}})^{\text{T}} \mathbf{C}_{\text{CMB}}^{-1} (\mathbf{A}_{\text{CMB,obs}} - \mathbf{A}_{\text{CMB,th}}), \quad (20)$$

with \mathbf{C}_{CMB} the covariance matrix provided in Tab. I in [65].

D. BAO

The latest BAO measurements, released by the DESI [60], are used in this paper. These data are obtained from more than 14 million galaxies and quasars drawn from the DESI

Parameter	Prior	Λ CDM	w CDM	w_0w_a CDM
$H_0(\text{km}/(\text{s} \cdot \text{Mpc}))$	(0, 150)	68.55 ± 0.30	68.09 ± 0.59	67.79 ± 0.59
Ω_{m0}	(0, 1)	0.3026 ± 0.0037	0.3059 ± 0.0051	0.3115 ± 0.0057
$\Omega_b h^2$	(0, 0.05)	0.02253 ± 0.00012	0.02256 ± 0.00013	0.02245 ± 0.00013
f_d	(0, 1)	$0.945^{+0.051}_{-0.017}$	$0.943^{+0.050}_{-0.020}$	≥ 0.936
$\text{DM}_{\text{halo}}^{\text{MW}}(\text{pc cm}^{-3})$	$\mathcal{N}(65, 15^2)$ in (50, 80)	≤ 55.6	≤ 55.6	≤ 55.6
$m_\gamma(\text{kg})$	(0, 2×10^{-49})	$\leq 4.83 \times 10^{-51}$	$\leq 4.71 \times 10^{-51}$	$\leq 4.86 \times 10^{-51}$
$w(w_0)$	(-3, 1)	-	-0.978 ± 0.024	-0.855 ± 0.056
w_a	(-3, 2)	-	-	$-0.52^{+0.23}_{-0.21}$

TABLE I. Summary of the MCMC parameters, their prior distributions, and posterior constraints by adopting the Λ CDM model, the w CDM model and the w_0w_a CDM model.

DR2. The extracted BAO signals, which expressed as $D_M(z)/r_s(z_d)$, $D_H(z)/r_s(z_d)$ and $D_V(z)/r_s(z_d)$, enable the measurement of key cosmological quantities, where $D_M(z)$, $D_H(z)$ and $D_V(z)$ are the transverse comoving distance, the Hubble horizon, and the angle-averaged distance, respectively, and $r_s(z_d)$ is the sound horizon at the drag epoch $z_d = 1059.94$ [64]. In a spatially flat universe, the transverse comoving distance, the Hubble horizon and the angle-averaged distance respectively take the forms:

$$D_M(z) = \frac{c}{H_0} \int_0^z \frac{dz'}{\tilde{E}(z')}, \quad D_H(z) = \frac{c}{H_0 \tilde{E}(z)}, \quad D_V(z) = \left[\frac{cz}{H_0} \frac{D_M^2(z)}{\tilde{E}(z)} \right]^{1/3}. \quad (21)$$

Defining $\mathbf{A}_{\text{BAO}} = \{D_M(z)/r_s(z_d), D_H(z)/r_s(z_d), D_V(z)/r_s(z_d)\}$, we can express the log-likelihood function of BAO datasets as

$$\ln \mathcal{L}_{\text{BAO}} \propto -\frac{1}{2} (\mathbf{A}_{\text{BAO,obs}} - \mathbf{A}_{\text{BAO,th}})^T \mathbf{C}_{\text{BAO}}^{-1} (\mathbf{A}_{\text{BAO,obs}} - \mathbf{A}_{\text{BAO,th}}) \quad (22)$$

with the $\mathbf{A}_{\text{BAO,obs}}$ and the covariance matrix \mathbf{C}_{BAO} shown in Tab. IV in [60].

When the FRB, SN Ia, CMB and BAO are considered together, the posterior distributions for free parameters can be acquired by maximizing the joint log-likelihood function:

$$\ln \mathcal{L}_{\text{total}} = \sum_i \ln \mathcal{L}_i, \quad i = \text{FRB, SN Ia, CMB, BAO}. \quad (23)$$

We employ emcee python package [83] for applying Markov Chain Monte Carlo (MCMC) process, based on the joint log-likelihood function given in Eq. (23). The priors for all parameters are listed in the second column of Tab. I.

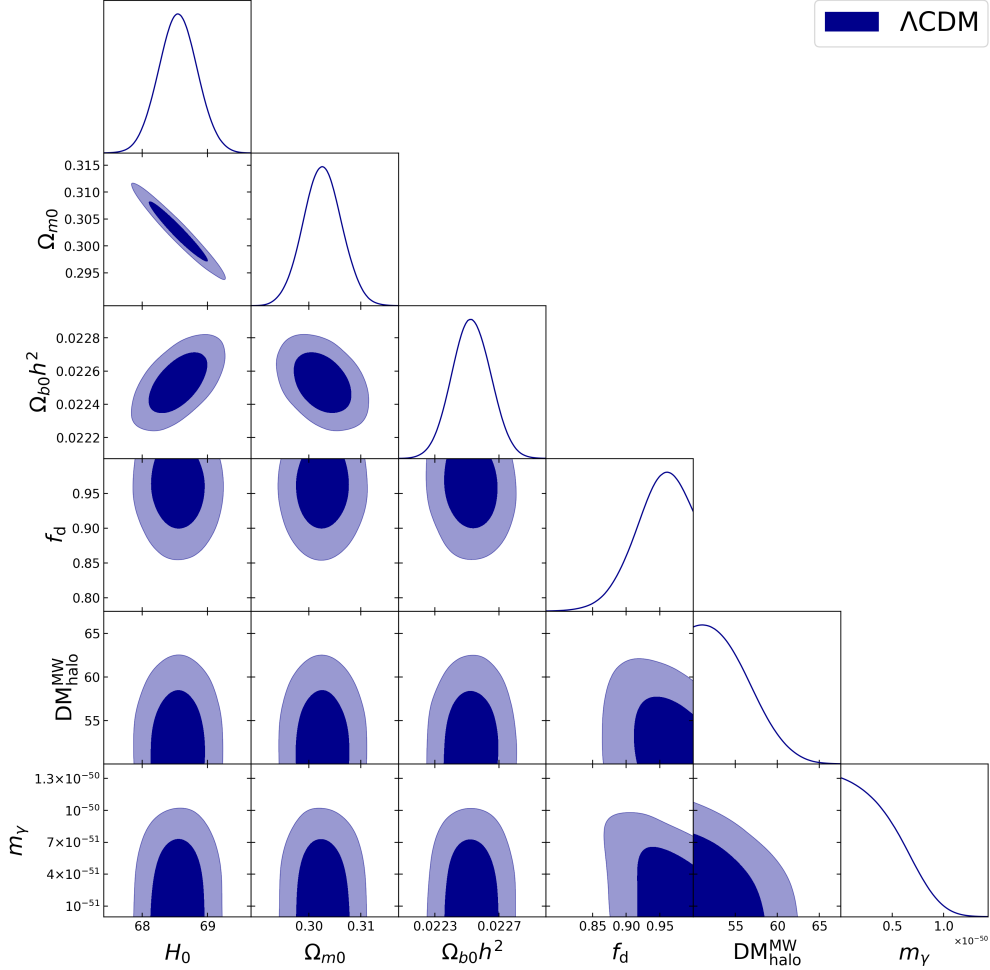


FIG. 1. 1D marginalized posterior distribution and 2D 1-2 σ contour regions for totally parameters constrained by a combination of FRB, CMB, BAO and SN Ia in the Λ CDM model.

IV. RESULTS

Within the framework of three cosmological models, we run 32 independent Markov Chain Monte Carlo (MCMC) chains for each model. The number of iterations (N_{steps}) for each chain is automatically controlled by the sampler. Convergence is assessed using the integrated autocorrelation time τ for all parameters, with the stopping criterion: (1) $N_{\text{steps}} > 50 \times \tau$ and (2) $|\frac{\tau_{\text{old}} - \tau}{\tau}| < 0.01$, where τ_{old} is the value from the previous checkpoint. The convergence test is performed every 1,000 iterations.

In the context of the Λ CDM model, the constraints on cosmological parameters and the photon mass are presented in Fig. 1 and summarized in Tab. I. The combined FRB, SN Ia, CMB and BAO yield tight constraints on the key cosmological parameters: $H_0 =$

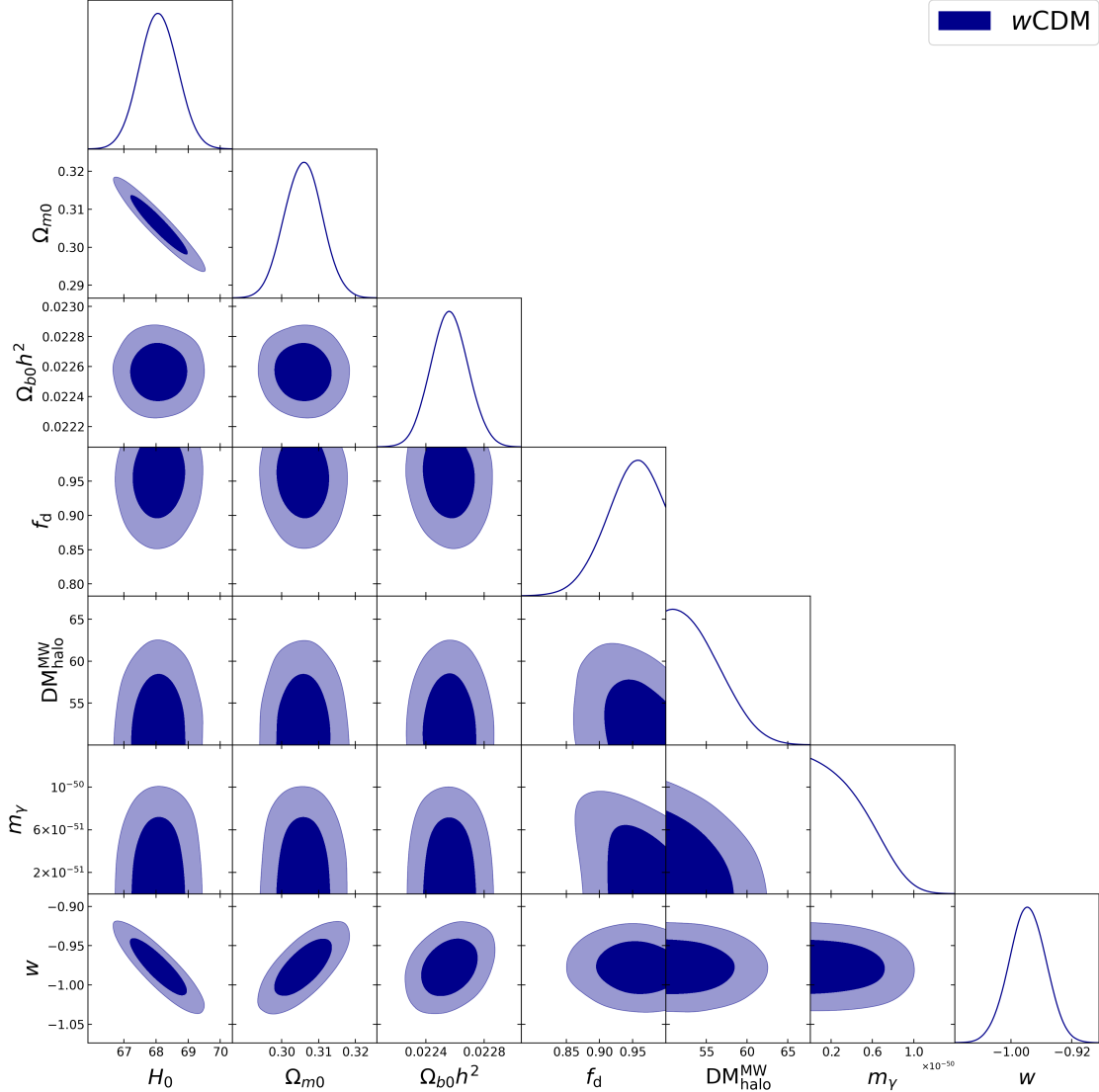


FIG. 2. Constraints on photon mass and free parameters in the w CDM model.

68.55 ± 0.30 km/(s · Mpc), $\Omega_{m0} = 0.3026 \pm 0.0037$ and $\Omega_{b0}h^2 = 0.02253 \pm 0.00012$ at the 1σ CL. These results are well consistent with previous determinations from Planck 2018, DESI, and ACT [60, 64, 84]. The baryon fraction in the diffuse state is constrained to $f_d = 0.945^{+0.051}_{-0.017}$ and the Milky Way halo dispersion measure satisfies $\text{DM}_{\text{halo}}^{\text{MW}} \leq 55.6$ at the 1σ CL. Most importantly, we obtain an upper limit on the photon mass: 4.83×10^{-51} kg at the 1σ CL.

Fig. 2 and Tab. I illustrate the constraints when the w CDM model is adopted. Compared to Λ CDM, the constraints on H_0 , Ω_{m0} , $\Omega_{b0}h^2$, f_d and $\text{DM}_{\text{halo}}^{\text{MW}}$ change only slightly. The equation of state w for dark energy is $w = -0.978 \pm 0.024$ which is marginally above -1 , though $w = -1$ remains allowed at the 1σ CL. The photon mass constraint slightly improves

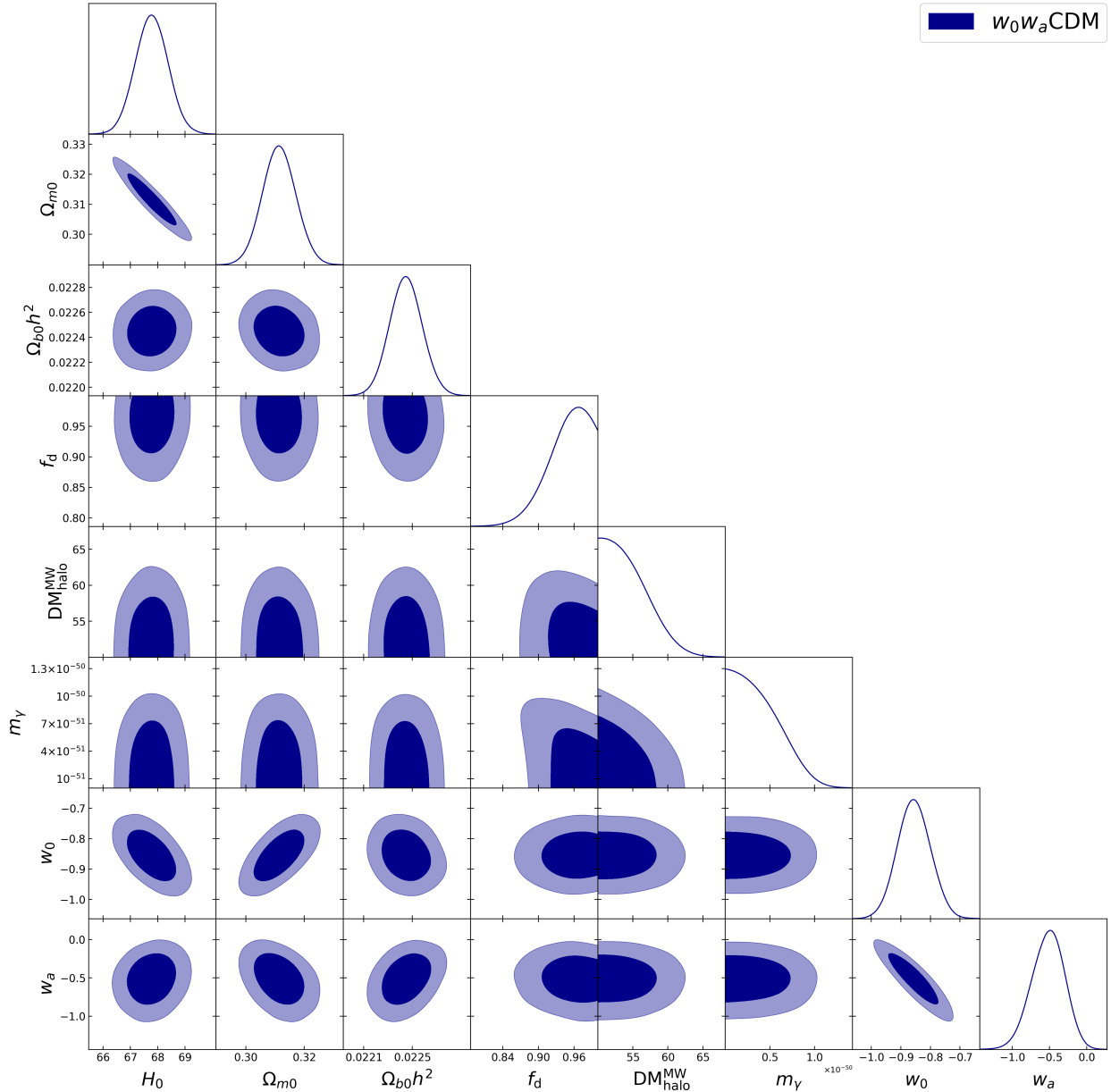


FIG. 3. Constraints on photon mass and free parameters in the w_0w_a CDM model.

to $m_\gamma < 4.71 \times 10^{-51}$ kg, smaller than 4.83×10^{-51} kg obtained in the Λ CDM model. Even with one additional free parameter relative to Λ CDM, the limit is essentially unchanged, indicating that the photon mass constraint is robust.

We next consider the Chevallier-Polarski-Linder (CPL) parametrization of dark energy, with an evolving equation of state $w(a) = w_0 + w_a(1 - a)$. Results are shown in Fig. 3 and Tab. I. The constraints on H_0 , Ω_{m0} , $\Omega_{b0}h^2$, f_d and $\text{DM}_{\text{halo}}^{\text{MW}}$ remain consistent with those obtained in the Λ CDM and w CDM models. We find that the allowed region for w_a deviates from zero at more than 2σ , indicating that a preference for dynamical dark

Parameter	Prior	Λ CDM	w CDM	w_0w_a CDM
$H_0(\text{km}/(\text{s} \cdot \text{Mpc}))$	(0, 150)	68.56 ± 0.29	68.13 ± 0.58	67.84 ± 0.60
Ω_{m0}	(0, 1)	0.3026 ± 0.0037	0.3055 ± 0.0051	0.3111 ± 0.0057
$\Omega_b h^2$	(0, 0.05)	0.02253 ± 0.00012	0.02256 ± 0.00013	0.02245 ± 0.00013
f_d	(0, 1)	$0.922^{+0.056}_{-0.035}$	$0.921^{+0.057}_{-0.036}$	$0.927^{+0.060}_{-0.030}$
$\text{DM}_{\text{halo}}^{\text{MW}}(\text{pc cm}^{-3})$	$\mathcal{N}(65, 15^2)$ in (50, 80)	≤ 53.8	≤ 53.8	≤ 53.9
$m_\gamma(\text{kg})$	(0, 2×10^{-49})	$\leq 4.28 \times 10^{-51}$	$\leq 4.26 \times 10^{-51}$	$\leq 4.22 \times 10^{-51}$
$w(w_0)$	(-3, 1)	-	-0.980 ± 0.024	-0.856 ± 0.056
w_a	(-3, 2)	-	-	$-0.52^{+0.23}_{-0.21}$
μ_{host}	(3.40, 5.40)	$4.33^{+0.22}_{-0.18}$	$4.32^{+0.22}_{-0.18}$	$4.33^{+0.22}_{-0.18}$
σ_{host}	(0.5, 1.5)	$1.10^{+0.11}_{-0.16}$	$1.10^{+0.11}_{-0.16}$	$1.10^{+0.11}_{-0.16}$

TABLE II. Summary of the MCMC parameters, including μ_{host} and σ_{host} , their prior distributions, and posterior constraints for the Λ CDM, w CDM, and w_0w_a CDM models.

energy. In addition, the value of w_0 is noticeably larger than -1 , suggesting a lower present-day expansion rate of our universe than predicted by the Λ CDM model. These trends are consistent with recent DESI DR2 findings [60, 85–87]. The upper limit on the photon mass is 4.86×10^{-51} kg, differing only slightly from the values obtained in Λ CDM and w CDM. This result might indicate that the inferred photon mass exhibits little sensitivity to the assumed background cosmological model. We note, however, that this conclusion should be interpreted with some caution, as the current sample of localized FRBs is dominated by low-redshift sources, with only a small number located near $z \sim 1$.

To further assess the potential influence of the assumption inherited from the Λ CDM-based IllustrisTNG simulation, we additionally treat μ_{host} and σ_{host} as free parameters, with their respective priors being $\mu_{\text{host}} \in (3.40, 5.40)$ and $\sigma_{\text{host}} \in (0.5, 1.5)$. The results are summarized in Table II. The photon mass is constrained to $m_\gamma \leq 4.28 \times 10^{-51}$ kg, $m_\gamma \leq 4.26 \times 10^{-51}$ kg and $m_\gamma \leq 4.22 \times 10^{-51}$ kg in the contexts of Λ CDM, w CDM and w_0w_a CDM cosmologies, respectively. Compared with results in Tab. I, where μ_{host} and σ_{host} are derived from the IllustrisTNG simulation, we find that treating μ_{host} and σ_{host} as free parameters leads to only minor changes in the inferred photon-mass bounds, in fact yielding slightly tighter constraints. The variation in the baryon mass fraction f_d resulting from two

different treatments of μ_{host} and σ_{host} is non-negligible, with a smaller f_d obtained when μ_{host} and σ_{host} are treated as free parameters. By contrast, the remaining cosmological parameters, including H_0 , Ω_{m0} , $\Omega_b h^2$, $\text{DM}_{\text{halo}}^{\text{MW}}$, $w(w_0)$ and w_a , remain in good agreement with those derived using the IllustrisTNG-based priors.

V. CONCLUSIONS AND DISCUSSIONS

The DMs of cosmological and well-localized FRBs have become powerful tools for estimating cosmological parameters. In this paper, we first improved the DM distribution from extragalactic gas proposed in [38] by restoring a missing normalization factor and by allowing the parameters α and β in the probability distribution function for the DM of cosmic origin to vary with redshift. We then utilized this improved distribution to test whether the photon has a non-zero rest mass, since any such mass would contribute an additional effective DM term. Using 104 localized FRBs, combined with SN Ia, CMB, and BAO data, we obtain the following 1σ upper limits on the photon rest mass: $m_\gamma \leq 4.83 \times 10^{-51}$ kg for Λ CDM model, $m_\gamma \leq 4.71 \times 10^{-51}$ kg for the w CDM model and $m_\gamma \leq 4.86 \times 10^{-51}$ kg for the $w_0 w_a$ CDM model. These values differ only minimally among the three cosmological models. However, we refrain from concluding that the inferred photon mass is entirely insensitive to the assumed cosmological background, since the current FRB sample is dominated by low-redshift sources, with only a few localized near $z \sim 1$. We further assess the impact of the Λ CDM assumption adopted in the IllustrisTNG simulation by treating μ_{host} and σ_{host} as free parameters. In this case, the photon mass is constrained to $m_\gamma \leq 4.28 \times 10^{-51}$ kg, $m_\gamma \leq 4.26 \times 10^{-51}$ kg and $m_\gamma \leq 4.22 \times 10^{-51}$ kg within the Λ CDM, w CDM and $w_0 w_a$ CDM cosmologies, respectively. These constraints are slightly tighter than those obtained when μ_{host} and σ_{host} are fixed to the IllustrisTNG-based values. Overall, our analysis provides strong empirical support for the massless nature of the photon.

Fig. 4 compares our photon-mass constraints with previous FRB-based limits. Each cyan point represents an upper limit obtained in earlier studies [44–54, 57–59], while the three green points correspond to the upper limits obtained here. The red dashed line shows the average upper limit on m_γ across three cosmological models we considered. It is apparent that our results are weaker than previous values such as $m_\gamma \leq 3.1 \times 10^{-51}$ kg (from 129 FRBs, most of which lack redshift measurements [57]), $m_\gamma \leq 3.5 \times 10^{-51}$ kg [46] (from 32

well-localized FRBs using a cosmological-independent method to determine the luminosity distance), and $m_\gamma \leq 3.8 \times 10^{-51}$ kg [59] (from 32 well-localized FRBs with the cosmological parameters determined from the CMB, SNIa and BAO).

However, these earlier studies [46, 57, 59] employed the DM_{ext} distribution proposed by Macquart et al. [38], which omits an essential normalization factor $1/\langle DM_{\text{IGM}} \rangle$. As shown in recent analyses [76, 77], this omission significantly biases constraints on cosmological parameters. The tight limits obtained in [46, 57, 59], even with smaller datasets, further illustrate the impact of the missing normalization. Our analysis incorporates the corrected distribution and therefore provides more reliable constraints.

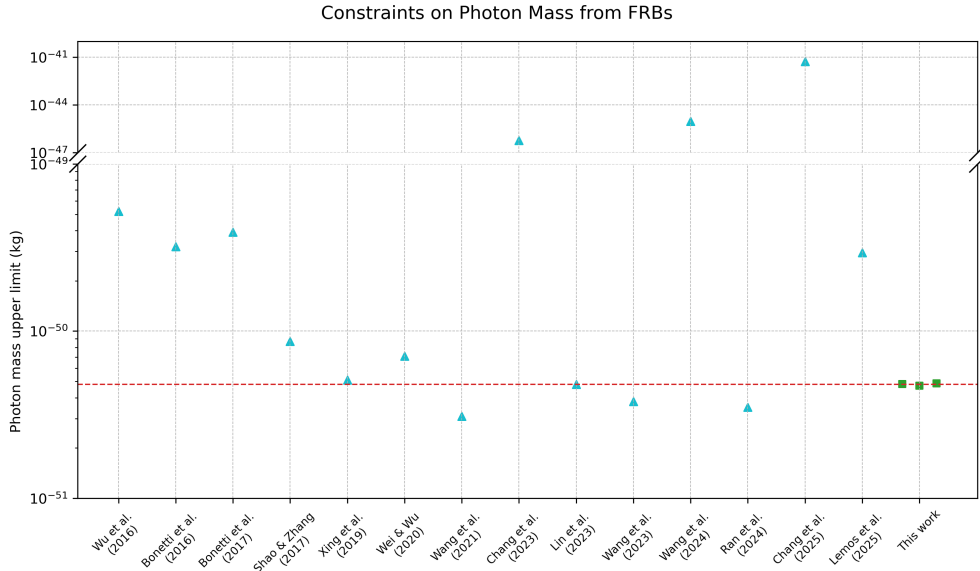


FIG. 4. The upper limits on the photon rest mass from FRBs, derived from both previous works and the current study, are presented. Cyan points represent constraints obtained from previous studies, while the three green ones correspond to our results within the framework of three different cosmological models. The red dashed line indicates the average upper limit on m_γ across the three cosmological models considered in this work.

ACKNOWLEDGMENTS

We appreciate very much the insightful comments and helpful suggestions by the anonymous referee. The authors Yuchen Zhang and Yang Liu make equal contributions to this work. This work was supported by the National Natural Science Foundation of China

(Grants No. 12275080 and No. 12075084), the Major basic research project of Hunan Province (Grant No. 2024JC0001), and the Innovative Research Group of Hunan Province (Grant No. 2024JJ1006).

- [1] A. Einstein, Zur Elektrodynamik bewegter Körper, [Annalen Phys.](#) **322**, 891 (1905).
- [2] E. R. Williams, J. E. Faller, and H. A. Hill, New experimental test of Coulomb's law: A Laboratory upper limit on the photon rest mass, [Phys. Rev. Lett.](#) **26**, 721 (1971).
- [3] N. M. Kroll, CONCENTRIC SPHERICAL CAVITIES AND LIMITS ON THE PHOTON REST MASS, [Phys. Rev. Lett.](#) **27**, 340 (1971).
- [4] M. A. Chernikov, C. J. Gerber, H. R. Ott, and H. J. Gerber, Low temperature upper limit of the photon mass: Experimental null test of Ampere's law, [Phys. Rev. Lett.](#) **68**, 3383 (1992), [Erratum: [Phys.Rev.Lett.](#) 69, 2999 (1992)].
- [5] R. Lakes, Experimental limits on the photon mass and cosmic magnetic vector potential, [Phys. Rev. Lett.](#) **80**, 1826 (1998).
- [6] J. Luo, L.-C. Tu, Z.-K. Hu, and E.-J. Luan, New experimental limit on the photon rest mass with a rotating torsion balance, [Phys. Rev. Lett.](#) **90**, 081801 (2003).
- [7] B. E. Schaefer, Severe limits on variations of the speed of light with frequency, [Phys. Rev. Lett.](#) **82**, 4964 (1999), [arXiv:astro-ph/9810479](#).
- [8] J.-J. Wei, E.-K. Zhang, S.-B. Zhang, and X.-F. Wu, New Limits on the Photon Mass with Radio Pulsars in the Magellanic Clouds, [Res. Astron. Astrophys.](#) **17**, 13 (2017), [arXiv:1608.07675 \[astro-ph.HE\]](#).
- [9] D. J. Bartlett, H. Desmond, P. G. Ferreira, and J. Jasche, Constraints on quantum gravity and the photon mass from gamma ray bursts, [Phys. Rev. D](#) **104**, 103516 (2021), [arXiv:2109.07850 \[gr-qc\]](#).
- [10] B. Lovell, F. L. Whipple, and L. H. Solomon, Relative velocity of light and radio waves in space, [Nature](#) **202**, 377 (1964).
- [11] B. Warner and R. E. Nather, Wavelength independence of the velocity of light in space, [Nature](#) **222**, 157 (1969).
- [12] B. Zhang, Y.-T. Chai, Y.-C. Zou, and X.-F. Wu, Constraining the mass of the photon with gamma-ray bursts, [JHEAp](#) **11**, 20 (2016).

- [13] J.-J. Wei and X.-F. Wu, Robust limits on photon mass from statistical samples of extragalactic radio pulsars, [JCAP **2018** \(07\), 045](#).
- [14] D. R. Lorimer, M. Bailes, M. A. McLaughlin, D. J. Narkevic, and F. Crawford, A bright millisecond radio burst of extragalactic origin, [Science **318**, 777 \(2007\)](#), [arXiv:0709.4301 \[astro-ph\]](#).
- [15] Z. Zheng, E. O. Ofek, S. R. Kulkarni, J. D. Neill, and M. Juric, Probing the Intergalactic Medium with Fast Radio Bursts, [Astrophys. J. **797**, 71 \(2014\)](#), [arXiv:1409.3244 \[astro-ph.HE\]](#).
- [16] M. Caleb, C. Flynn, and B. Stappers, Constraining the era of helium reionization using fast radio bursts, [Mon. Not. Roy. Astron. Soc. **485**, 2281 \(2019\)](#), [arXiv:1902.06981 \[astro-ph.HE\]](#).
- [17] P. Beniamini, P. Kumar, X. Ma, and E. Quataert, Exploring the epoch of hydrogen reionization using FRBs, [Mon. Not. Roy. Astron. Soc. **502**, 5134 \(2021\)](#), [arXiv:2011.11643 \[astro-ph.CO\]](#).
- [18] T. Hashimoto, T. Goto, T.-Y. Lu, A. Y. L. On, D. J. D. Santos, S. J. Kim, E. K. Eser, S. C. C. Ho, T. Y. Y. Hsiao, and L. Y. W. Lin, Revealing the cosmic reionization history with fast radio bursts in the era of Square Kilometre Array, [Mon. Not. Roy. Astron. Soc. **502**, 2346 \(2021\)](#), [arXiv:2101.08798 \[astro-ph.CO\]](#).
- [19] J.-J. Wei and C.-Y. Gao, Forecasts for Helium Reionization Detection with Fast Radio Bursts in the Era of Square Kilometre Array, [Astrophys. J. **975**, 184 \(2024\)](#), [arXiv:2409.01543 \[astro-ph.CO\]](#).
- [20] A. K. Shaw, R. Ghara, P. Beniamini, S. Zaroubi, and P. Kumar, Asking Fast Radio Bursts for More than Reionization History, [Astrophys. J. **993**, 209 \(2025\)](#), [arXiv:2409.03255 \[astro-ph.CO\]](#).
- [21] Z.-X. Li, H. Gao, X.-H. Ding, G.-J. Wang, and B. Zhang, Strongly lensed repeating fast radio bursts as precision probes of the universe, [Nature Commun. **9**, 3833 \(2018\)](#), [arXiv:1708.06357 \[astro-ph.CO\]](#).
- [22] S. Hagstotz, R. Reischke, and R. Lilow, A new measurement of the Hubble constant using fast radio bursts, [Mon. Not. Roy. Astron. Soc. **511**, 662 \(2022\)](#).
- [23] C. James, E. Ghosh, J. Prochaska, K. Bannister, S. Bhandari, C. Day, A. Deller, M. Glowacki, A. Gordon, K. Heintz, *et al.*, A measurement of hubble’s constant using fast radio bursts, [Mon. Not. Roy. Astron. Soc. **516**, 4862 \(2022\)](#).
- [24] Y. Liu, H. Yu, and P. Wu, Cosmological-model-independent Determination of Hubble Constant from Fast Radio Bursts and Hubble Parameter Measurements, [Astrophys. J. Lett. **946**, L49](#)

- (2023), [arXiv:2210.05202 \[astro-ph.CO\]](#).
- [25] J. A. S. Fortunato, D. J. Bacon, W. S. Hipólito-Ricaldi, and D. Wands, Fast Radio Bursts and Artificial Neural Networks: a cosmological-model-independent estimation of the Hubble constant, *JCAP* **2025** (01), 018, [arXiv:2407.03532 \[astro-ph.CO\]](#).
- [26] E. F. Piratova-Moreno, L. Á. García, C. A. Benavides-Gallego, and C. Cabrera, Fast Radio Bursts as cosmological proxies: estimating the Hubble constant, *arXiv* (2025), [arXiv:2502.08509 \[astro-ph.CO\]](#).
- [27] Q. Wu, G.-Q. Zhang, and F.-Y. Wang, An 8 per cent determination of the Hubble constant from localized fast radio bursts, *Mon. Not. Roy. Astron. Soc.* **515**, L1 (2022), [Erratum: *Mon.Not.Roy.Astron.Soc.* 531, L8 (2024)], [arXiv:2108.00581 \[astro-ph.CO\]](#).
- [28] L. Connor *et al.*, A gas-rich cosmic web revealed by the partitioning of the missing baryons, *Nature Astron.* **9**, 1226 (2025), [arXiv:2409.16952 \[astro-ph.CO\]](#).
- [29] T. Lemos, Estimating the baryon fraction in the IGM from well-localized FRBs and DESI data, *arXiv* (2025), [arXiv:2507.17693 \[astro-ph.CO\]](#).
- [30] Z. Li, H. Gao, J.-J. Wei, Y.-P. Yang, B. Zhang, and Z.-H. Zhu, Cosmology-insensitive estimate of IGM baryon mass fraction from five localized fast radio bursts, *Mon. Not. Roy. Astron. Soc.* **496**, L28 (2020), [arXiv:2004.08393 \[astro-ph.HE\]](#).
- [31] B. Wang and J.-J. Wei, An 8.0% Determination of the Baryon Fraction in the Intergalactic Medium from Localized Fast Radio Bursts, *Astrophys. J.* **944**, 50 (2023), [arXiv:2211.02209 \[astro-ph.CO\]](#).
- [32] W. Deng and B. Zhang, Cosmological Implications of Fast Radio Burst/Gamma-Ray Burst Associations, *Astrophys. J. Lett.* **783**, L35 (2014), [arXiv:1401.0059 \[astro-ph.HE\]](#).
- [33] V. Ravi, Measuring the Circumgalactic and Intergalactic Baryon Contents with Fast Radio Bursts, *Astrophys. J.* **872**, 88 (2019), [arXiv:1804.07291 \[astro-ph.HE\]](#).
- [34] J. B. Muñoz and A. Loeb, Finding the Missing Baryons with Fast Radio Bursts and Sunyaev-Zeldovich Maps, *Phys. Rev. D* **98**, 103518 (2018), [arXiv:1809.04074 \[astro-ph.CO\]](#).
- [35] Z. Li, H. Gao, J.-J. Wei, Y.-P. Yang, B. Zhang, and Z.-H. Zhu, Cosmology-independent estimate of the fraction of baryon mass in the IGM from fast radio burst observations, *Astrophys. J.* **876**, 146 (2019), [arXiv:1904.08927 \[astro-ph.CO\]](#).
- [36] A. Walters, Y.-Z. Ma, J. Sievers, and A. Weltman, Probing Diffuse Gas with Fast Radio Bursts, *Phys. Rev. D* **100**, 103519 (2019), [arXiv:1909.02821 \[astro-ph.CO\]](#).

- [37] J.-J. Wei, Z. Li, H. Gao, and X.-F. Wu, Constraining the Evolution of the Baryon Fraction in the IGM with FRB and $H(z)$ data, *JCAP* **2019** (09), 039, [arXiv:1907.09772 \[astro-ph.CO\]](#).
- [38] J. P. Macquart *et al.*, A census of baryons in the Universe from localized fast radio bursts, *Nature* **581**, 391 (2020), [arXiv:2005.13161 \[astro-ph.CO\]](#).
- [39] K. B. Yang, Q. Wu, and F. Y. Wang, Finding the Missing Baryons in the Intergalactic Medium with Localized Fast Radio Bursts, *Astrophys. J. Lett.* **940**, L29 (2022), [arXiv:2211.04058 \[astro-ph.HE\]](#).
- [40] H.-N. Lin and R. Zou, Probing the baryon mass fraction in IGM and its redshift evolution with fast radio bursts using Bayesian inference method, *Mon. Not. Roy. Astron. Soc.* **520**, 6237 (2023), [arXiv:2302.10585 \[astro-ph.CO\]](#).
- [41] Y. Liu, Y. Zhang, H. Yu, and P. Wu, Constraining the Baryon Fraction in the Intergalactic Medium with 92 localized Fast Radio Bursts, *arXiv* (2025), [arXiv:2506.03536 \[astro-ph.CO\]](#).
- [42] J.-G. Zhang, J.-Y. Song, Z.-W. Zhao, W.-P. Sun, J.-F. Zhang, and X. Zhang, Measuring cosmic baryon density with FRB and GW data, *arXiv* (2025), [arXiv:2507.06841 \[astro-ph.CO\]](#).
- [43] M. J. Bentum, L. Bonetti, and A. D. A. M. Spallicci, Dispersion by pulsars, magnetars, fast radio bursts and massive electromagnetism at very low radio frequencies, *Adv. Space Res.* **59**, 736 (2017), [arXiv:1607.08820 \[astro-ph.IM\]](#).
- [44] T. Lemos, R. Gonçalves, J. Carvalho, and J. Alcaniz, Cosmological model-independent limits on photon mass from FRB and SNe data, *JCAP* **2025** (11), 019, [arXiv:2504.21129 \[astro-ph.CO\]](#).
- [45] C.-M. Chang, J.-J. Wei, K.-L. Meng, S.-B. Zhang, H.-X. Gao, J.-J. Geng, and X.-F. Wu, Bounding the photon mass with gravitationally lensed fast radio bursts, *Phys. Rev. D* **111**, L041304 (2025), [arXiv:2412.09806 \[astro-ph.HE\]](#).
- [46] J.-Y. Ran, B. Wang, and J.-J. Wei, Cosmology-Independent Photon Mass Limits from Localized Fast Radio Bursts by Using Artificial Neural Networks, *Chin. Phys. Lett.* **41**, 059501 (2024), [arXiv:2404.17154 \[astro-ph.CO\]](#).
- [47] Y.-B. Wang, X. Zhou, A. Kurban, and F.-Y. Wang, Bounding the Photon Mass with Ultrawide Bandwidth Pulsar Timing Data and Dedispersed Pulses of Fast Radio Bursts, *Astrophys. J.* **965**, 38 (2024), [arXiv:2403.06422 \[astro-ph.HE\]](#).
- [48] L. Shao and B. Zhang, Bayesian framework to constrain the photon mass with a catalog of fast radio bursts, *Phys. Rev. D* **95**, 123010 (2017), [arXiv:1705.01278 \[hep-ph\]](#).

- [49] X.-F. Wu, S.-B. Zhang, H. Gao, J.-J. Wei, Y.-C. Zou, W.-H. Lei, B. Zhang, Z.-G. Dai, and P. Mészáros, Constraints on the Photon Mass with Fast Radio Bursts, *Astrophys. J. Lett.* **822**, L15 (2016), [arXiv:1602.07835 \[astro-ph.HE\]](#).
- [50] J.-J. Wei and X.-F. Wu, Combined Limit on the Photon Mass with Nine Localized Fast Radio Bursts, *Astron. Astrophys.* **20**, 206 (2020), [arXiv:2006.09680 \[astro-ph.HE\]](#).
- [51] L. Bonetti, J. Ellis, N. E. Mavromatos, A. S. Sakharov, E. K. G. Sarkisyan-Grinbaum, and A. D. A. M. Spallicci, Photon Mass Limits from Fast Radio Bursts, *Phys. Lett. B* **757**, 548 (2016), [arXiv:1602.09135 \[astro-ph.HE\]](#).
- [52] L. Bonetti, J. Ellis, N. E. Mavromatos, A. S. Sakharov, E. K. Sarkisyan-Grinbaum, and A. D. A. M. Spallicci, FRB 121102 Casts New Light on the Photon Mass, *Phys. Lett. B* **768**, 326 (2017), [arXiv:1701.03097 \[astro-ph.HE\]](#).
- [53] N. Xing, H. Gao, J. Wei, Z. Li, W. Wang, B. Zhang, X.-F. Wu, and P. Mészáros, Limits on the Weak Equivalence Principle and Photon Mass with FRB 121102 Subpulses, *Astrophys. J. Lett.* **882**, L13 (2019), [arXiv:1907.00583 \[astro-ph.HE\]](#).
- [54] C.-M. Chang, J.-J. Wei, S.-B. Zhang, and X.-F. Wu, Bounding the photon mass with the dedispersed pulses of the Crab pulsar and FRB 180916B, *JCAP* **2023** (01), 010, [Erratum: *JCAP* 07, E01 (2024)], [arXiv:2207.00950 \[astro-ph.HE\]](#).
- [55] Z. J. Zhang, K. Yan, C. M. Li, G. Q. Zhang, and F. Y. Wang, Intergalactic medium dispersion measures of fast radio bursts estimated from IllustrisTNG simulation and their cosmological applications, *Astrophys. J.* **906**, 49 (2021), [arXiv:2011.14494 \[astro-ph.CO\]](#).
- [56] R. M. Konietzka, L. Connor, V. A. Semenov, A. Beane, V. Springel, and L. Hernquist, Ray-tracing Fast Radio Bursts Through IllustrisTNG: Cosmological Dispersion Measures from Redshift 0 to 5.5, *arXiv* (2025), [arXiv:2507.07090 \[astro-ph.CO\]](#).
- [57] H. Wang, X. Miao, and L. Shao, Bounding the photon mass with cosmological propagation of fast radio bursts, *Phys. Lett. B* **820**, 136596 (2021), [arXiv:2103.15299 \[astro-ph.HE\]](#).
- [58] H.-N. Lin, L. Tang, and R. Zou, Revised constraints on the photon mass from well-localized fast radio bursts, *Mon. Not. Roy. Astron. Soc.* **520**, 1324 (2023), [arXiv:2301.12103 \[gr-qc\]](#).
- [59] B. Wang, J.-J. Wei, X.-F. Wu, and M. López-Corredoira, Revisiting constraints on the photon rest mass with cosmological fast radio bursts, *JCAP* **2023** (09), 025, [arXiv:2304.14784 \[astro-ph.HE\]](#).
- [60] M. Abdul Karim *et al.* (DESI), DESI DR2 results. II. Measurements of baryon acoustic os-

- cillations and cosmological constraints, *Phys. Rev. D* **112**, 083515 (2025), [arXiv:2503.14738 \[astro-ph.CO\]](#).
- [61] M. Chevallier and D. Polarski, Accelerating universes with scaling dark matter, *Int. J. Mod. Phys. D* **10**, 213 (2001), [arXiv:gr-qc/0009008](#).
- [62] E. V. Linder, Exploring the expansion history of the universe, *Phys. Rev. Lett.* **90**, 091301 (2003), [arXiv:astro-ph/0208512](#).
- [63] D. Scolnic *et al.*, The Pantheon+ Analysis: The Full Data Set and Light-curve Release, *Astrophys. J.* **938**, 113 (2022), [arXiv:2112.03863 \[astro-ph.CO\]](#).
- [64] N. Aghanim *et al.* (Planck), Planck 2018 results. VI. Cosmological parameters, *Astron. Astrophys.* **641**, A6 (2020), [Erratum: *Astron. Astrophys.* 652, C4 (2021)], [arXiv:1807.06209 \[astro-ph.CO\]](#).
- [65] L. Chen, Q.-G. Huang, and K. Wang, Distance Priors from Planck Final Release, *JCAP* **2019** (02), 028, [arXiv:1808.05724 \[astro-ph.CO\]](#).
- [66] K. Ioka, Cosmic dispersion measure from gamma-ray burst afterglows: probing the reionization history and the burst environment, *Astrophys. J. Lett.* **598**, L79 (2003), [arXiv:astro-ph/0309200](#).
- [67] S. Inoue, Probing the cosmic reionization history and local environment of gamma-ray bursts through radio dispersion, *Mon. Not. Roy. Astron. Soc.* **348**, 999 (2004), [arXiv:astro-ph/0309364](#).
- [68] J. X. Prochaska and Y. Zheng, Probing galactic haloes with fast radio bursts, *Mon. Not. Roy. Astron. Soc.* **485**, 648 (2019).
- [69] M. McQuinn, Locating the "missing" baryons with extragalactic dispersion measure estimates, *Astrophys. J. Lett.* **780**, L33 (2014), [arXiv:1309.4451 \[astro-ph.CO\]](#).
- [70] G. D. Becker, J. S. Bolton, M. G. Haehnelt, and W. L. W. Sargent, Detection of Extended He II Reionization in the Temperature Evolution of the Intergalactic Medium, *Mon. Not. Roy. Astron. Soc.* **410**, 1096 (2011), [arXiv:1008.2622 \[astro-ph.CO\]](#).
- [71] A. A. Meiksin, The Physics of the Intergalactic Medium, *Rev. Mod. Phys.* **81**, 1405 (2009), [arXiv:0711.3358 \[astro-ph\]](#).
- [72] J. M. Cordes and T. J. W. Lazio, NE2001. 1. A New model for the galactic distribution of free electrons and its fluctuations, *arXiv* (2002), [arXiv:astro-ph/0207156](#).
- [73] J. M. Yao, R. N. Manchester, and N. Wang, A new Electron-density Model for Estimation of

- Pulsar and frb Distances, *Astrophys. J.* **835**, 29 (2017).
- [74] V. Ravi *et al.* (Deep Synoptic Array Team), Deep Synoptic Array Science: A 50 Mpc Fast Radio Burst Constrains the Mass of the Milky Way Circumgalactic Medium, *Astron. J.* **169**, 330 (2025), [arXiv:2301.01000 \[astro-ph.GA\]](#).
- [75] Y. Liu, B. Wang, P. Wu, J.-J. Wei, and X.-F. Wu, Investigating the Anisotropy of Dispersion Measure Contribution from the Galactic Halo by Using Fast Radio Bursts, *arXiv* (2026), [arXiv:2601.02849 \[astro-ph.GA\]](#).
- [76] Y. Zhang, Y. Liu, H. Yu, and P. Wu, Probability density function for dispersion measure of fast radio burst from extragalactic medium, *Phys. Rev. D* **112**, 083516 (2025), [arXiv:2504.06845 \[astro-ph.CO\]](#).
- [77] J. Zhuge, M. Kalomenopoulos, and B. Zhang, Hubble constant constraint using 117 FRBs with a more accurate probability density function for DM_{diff} , *arXiv* (2025), [arXiv:2508.05161 \[astro-ph.CO\]](#).
- [78] G. Q. Zhang, H. Yu, J. H. He, and F. Y. Wang, Dispersion measures of fast radio burst host galaxies derived from IllustrisTNG simulation, *Astrophys. J.* **900**, 170 (2020), [arXiv:2007.13935 \[astro-ph.HE\]](#).
- [79] C. W. James, J. X. Prochaska, J. P. Macquart, F. O. North-Hickey, K. W. Bannister, and A. Dunning, The z -DM distribution of fast radio bursts, *Mon. Not. Roy. Astron. Soc.* **509**, 4775 (2021), [arXiv:2101.08005 \[astro-ph.HE\]](#).
- [80] D. H. Gao, Q. Wu, J. P. Hu, S. X. Yi, X. Zhou, F. Y. Wang, and Z. G. Dai, Measuring Hubble constant using localized and unlocalized fast radio bursts, *Astron. Astrophys.* **698**, A215 (2025), [arXiv:2410.03994 \[astro-ph.CO\]](#).
- [81] K. Sharma *et al.*, Preferential occurrence of fast radio bursts in massive star-forming galaxies, *Nature* **635**, 61 (2024), [arXiv:2409.16964 \[astro-ph.HE\]](#).
- [82] D. Brout *et al.*, The Pantheon+ Analysis: Cosmological Constraints, *Astrophys. J.* **938**, 110 (2022), [arXiv:2202.04077 \[astro-ph.CO\]](#).
- [83] D. Foreman-Mackey, D. W. Hogg, D. Lang, and J. Goodman, emcee: The MCMC Hammer, *Publ. Astron. Soc. Pac.* **125**, 306 (2013), [arXiv:1202.3665 \[astro-ph.IM\]](#).
- [84] T. Louis *et al.* (ACT), The Atacama Cosmology Telescope: DR6 Power Spectra, Likelihoods and Λ CDM Parameters, *arXiv* (2025), [arXiv:2503.14452 \[astro-ph.CO\]](#).
- [85] S. Feng, Y. Gong, X. Liu, J.-H. Yan, and X. Chen, Constraining and Comparing the Dynamical

Dark Energy and f(R) Modified Gravity Models with Cosmological Distance Measurements, arXiv (2025), [arXiv:2510.23105 \[astro-ph.CO\]](#).

- [86] A. Smith, E. Özlüker, E. Di Valentino, and C. van de Bruck, Dynamical Dark Energy Meets Varying Electron Mass: Implications for Phantom Crossing and the Hubble Constant, arXiv (2025), [arXiv:2510.21931 \[astro-ph.CO\]](#).
- [87] K. Lodha *et al.* (DESI), Extended dark energy analysis using DESI DR2 BAO measurements, *Phys. Rev. D* **112**, 083511 (2025), [arXiv:2503.14743 \[astro-ph.CO\]](#).
- [88] P. Virtanen *et al.*, SciPy 1.0: Fundamental Algorithms for Scientific Computing in Python, *Nature Methods* **17**, 261 (2020).

Appendix A: Modified probability distribution function of Δ

Since the distribution of free electrons in the IGM is inhomogeneous, the actual value of DM_{cosmic} fluctuates around its average value $\langle DM_{\text{cosmic}} \rangle$. To account for this variation, Macquart *et al.* [38] introduced $\Delta = DM_{\text{cosmic}} / \langle DM_{\text{cosmic}} \rangle$ and proposed a probability distribution function (*Macquart distribution*) for Δ

$$P_{\text{cosmic}}(\Delta) = A\Delta^{-\beta} \exp \left[-\frac{(\Delta^{-\alpha} - C_0)^2}{2\alpha^2\sigma_{\text{cosmic}}^2} \right]. \quad (\text{A1})$$

Here both α and β are fixed to 3, A is the normalization constant, C_0 is a parameter determined by the requirement that the mean value of Δ equals 1, and σ_{cosmic} is assumed to follow $\sigma_{\text{cosmic}} = Fz^{-1/2}$ with F being treated as a free parameter. Later, Zhang *et al.* [55] treated σ_{cosmic} in Eq. (A1) as a free parameter and employed the IllustrisTNG cosmic simulation to determine the optimal values for different redshift points. Their results have since been widely adopted in subsequent studies. Recently, Konietzka *et al.* [56] proposed a new method for measuring DM_{cosmic} in the IllustrisTNG cosmic simulation and found Zhang *et al.* [55] had misestimated the standard deviation and higher moments of the DM_{cosmic} distribution by over 50%. Based on the continuous DM_{cosmic} catalog acquired through their new method, Konietzka *et al.* [56] found that the PDF of DM_{cosmic} takes a form similar to that of Eq. (A1), with parameters $\alpha \approx 1$ and $\beta \approx 3.3$ (*Konietzka distribution*), which fits well with their simulation data. However, since the Konietzka distribution [56] does not explicitly include the average $\langle DM_{\text{cosmic}} \rangle$, which encodes cosmological information, it is therefore incapable of using in FRB cosmology.

To address this problem, we assume that $P_{\text{cosmic}}(\Delta)$ takes a form similar as Eq. (A1), but C_0 is fixed to 1,

$$P_{\text{cosmic}}(\Delta) = A\Delta^{-\beta} \exp \left[-\frac{(\Delta^{-\alpha} - 1)^2}{2\alpha^2\sigma_{\text{cosmic}}^2} \right]. \quad (\text{A2})$$

Since Konietzka et al. [56] found that α and β taking values different from $\alpha = \beta = 3$ provide better fit, we treat α and β as free parameters and determine their values using the continuous $\text{DM}_{\text{cosmic}}$ catalog. In Eq. (A2), σ_{cosmic} is also assumed to a free parameter, determined along with α and β . To derive the values of α , β and σ_{cosmic} , we first calculate the $\langle \text{DM}_{\text{cosmic}} \rangle$ from Eq. (10) for each redshift points, adopting $H_0 = 67.74 \text{ km/s} \cdot \text{Mpc}^{-1}$, $\Omega_{m0} = 0.3089$, $\Omega_{b0} = 0.0486$ and $f_{eb} = f_d \cdot \chi_e = 0.83$, which are consistent with the assumptions made in generating the continuous catalog in [56]. Next, we employ a MCMC process to determine α , β and σ_{cosmic} by fitting $P(\text{DM}_{\text{cosmic}})$ to the simulated $\text{DM}_{\text{cosmic}}$ distribution. Here we emphasize that the PDF for $\text{DM}_{\text{cosmic}}$ is given by $P(\text{DM}_{\text{cosmic}}) = \frac{1}{\langle \text{DM}_{\text{cosmic}} \rangle} P_{\text{cosmic}}(\Delta)$ as investigated in [76, 77]. The obtained parameters values for each redshift point are listed in Table. III. In Fig. 5, we plot the variation of α , β , and σ_{cosmic} with redshift. These parameters exhibit more significant variations at low redshift, while their evolution becomes flatter at higher redshifts. Therefore, we adopt finer redshift intervals at low z and coarser intervals at high z .

To evaluate the validity of $P(\text{DM}_{\text{cosmic}})$ proposed here, we apply the Kolmogorov–Smirnov (KS) test through using the SciPy python package [88]. The KS test is defined as,

$$D_n(p) = \sup_x |F_p(x) - F_n(x)|, \quad (\text{A3})$$

where $F_p(x)$ and $F_n(x)$ are cumulative distribution functions (CDFs) corresponding to $P(\text{DM}_{\text{cosmic}})$ and the simulated $\text{DM}_{\text{cosmic}}$ distribution, respectively. The KS statistic $D_n(p)$ quantifies how far the samples deviate from the expected PDF. The KS test has a null hypothesis that the samples are drawn from $P(\text{DM}_{\text{cosmic}})$. We reject the null hypothesis if the difference $D_n(p)$ exceeds a critical value D_{crit} , which can be calculated as $D_{\text{crit}} \approx \frac{c(\tilde{\alpha})}{\sqrt{n}}$, where $\tilde{\alpha}$ is the significance level that represents the probability of wrongly rejecting a true null hypothesis, and n is the number of samples. For a specific redshift point, the continuous catalog has 120000 $\text{DM}_{\text{cosmic}}$ samples, and we adopt $\tilde{\alpha} = 0.05$ by convention. Thus we obtain $c(\tilde{\alpha}) = 1.36$ (from *Real Statistics Using Excel*²), leading to $D_{\text{crit}} \approx 0.0039$. After applying

² <https://real-statistics.com/statistics-tables/kolmogorov-smirnov-table/>

the KS test to $P(\text{DM}_{\text{cosmic}})$ with the parameters listed in Table. III, we plot the KS statistics for each redshift point in Fig. 6. The mean value of the KS statistic is 0.0042, which slightly exceeds the D_{crit} . We also include the KS statistics of the Macquart distribution [38] and the Konietzka distribution [56] in Fig. 6. It is evident that the PDF in [56] performs better than the one in [38], which is consistent with the finding reported in [56]. However, the KS statistics for both distributions clearly exceed D_{crit} , indicating that they are inadequate for describing the distribution of $\text{DM}_{\text{cosmic}}$. Furthermore, we find that the parameter F in Eq. (A1) varies from 1.15 to 0.16 as the redshift changes from 0.1 to 3.0, suggesting that F should not be treated as a constant. This implies that the relation $\sigma_{\text{cosmic}} = Fz^{-1/2}$ may be unsuitable.

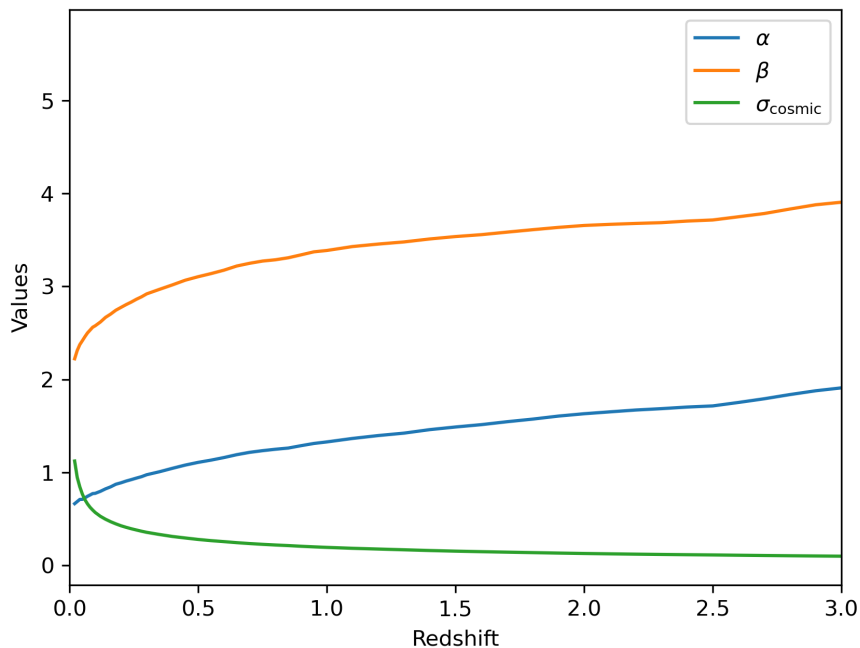


FIG. 5. Variations of α , β and σ_{cosmic} with redshift z .

z	α	β	σ_{cosmic}	A
0.02	0.6647	2.2223	1.1232	0.3612
0.03	0.6876	2.3111	0.9473	0.4235
0.04	0.7104	2.3746	0.8462	0.4726
0.05	0.7113	2.4166	0.7675	0.5174
0.06	0.7270	2.4599	0.7073	0.5610
0.07	0.7444	2.5001	0.6623	0.5992
0.08	0.7584	2.5305	0.6259	0.6344
0.09	0.7731	2.5611	0.5966	0.6658
0.10	0.7759	2.5770	0.5701	0.6963
0.12	0.7973	2.6172	0.5292	0.7509
0.14	0.8240	2.6674	0.4974	0.7997
0.16	0.8458	2.7028	0.4708	0.8458
0.18	0.8737	2.7439	0.4481	0.8902
0.20	0.8892	2.7745	0.4275	0.9331
0.22	0.9077	2.8045	0.4107	0.9719
0.24	0.9232	2.8317	0.3954	1.0099
0.26	0.9396	2.8620	0.3818	1.0459
0.28	0.9550	2.8882	0.3686	1.0837
0.30	0.9759	2.9199	0.3568	1.1202
0.35	1.0083	2.9690	0.3334	1.1997
0.40	1.0449	3.0165	0.3123	1.2823
0.45	1.0797	3.0669	0.2960	1.3534
0.50	1.1087	3.1045	0.2803	1.4298
0.55	1.1329	3.1378	0.2674	1.4991
0.60	1.1605	3.1743	0.2569	1.5611
0.65	1.1916	3.2193	0.2457	1.6325
0.70	1.2165	3.2487	0.2361	1.6991

z	α	β	σ_{cosmic}	A
0.75	1.2344	3.2725	0.2279	1.7608
0.80	1.2497	3.2864	0.2206	1.8185
0.85	1.2625	3.3078	0.2143	1.8716
0.90	1.2882	3.3393	0.2069	1.9388
0.95	1.3122	3.3718	0.2006	1.9999
1.00	1.3286	3.3863	0.1950	2.0579
1.10	1.3659	3.4286	0.1851	2.1684
1.20	1.3969	3.4552	0.1771	2.2661
1.30	1.4230	3.4781	0.1692	2.3720
1.40	1.4607	3.5101	0.1613	2.4883
1.50	1.4890	3.5360	0.1545	2.5970
1.60	1.5141	3.5563	0.1489	2.6954
1.70	1.5454	3.5835	0.1437	2.7913
1.80	1.5738	3.6096	0.1387	2.8922
1.90	1.6063	3.6345	0.1338	2.9988
2.00	1.6316	3.6552	0.1294	3.0988
2.10	1.6517	3.6672	0.1256	3.1941
2.20	1.6714	3.6770	0.1222	3.2824
2.30	1.6861	3.6853	0.1191	3.3671
2.40	1.7033	3.7024	0.1163	3.4484
2.50	1.7155	3.7142	0.1138	3.5240
2.60	1.7529	3.7486	0.1106	3.6232
2.70	1.7924	3.7834	0.1077	3.7209
2.80	1.8375	3.8319	0.1050	3.8168
2.90	1.8784	3.8776	0.1026	3.9077
3.00	1.9096	3.9050	0.1003	3.9963

TABLE III. Optimal values of parameters in $P_{\text{cosmic}}(\Delta)$ based on the continuous catalog.

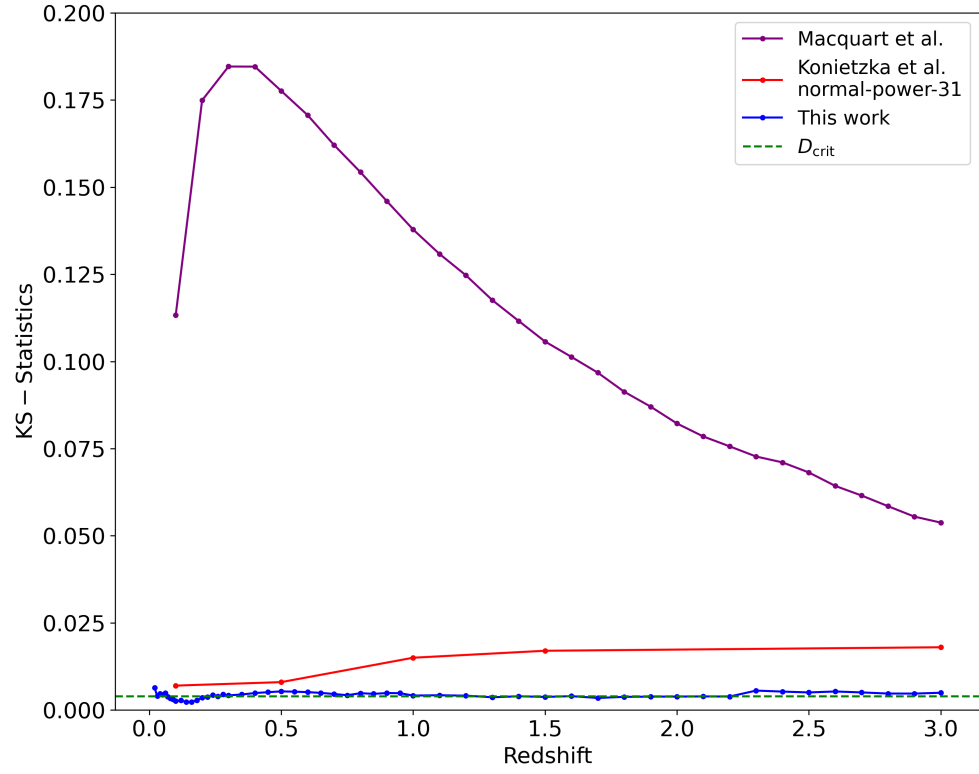


FIG. 6. The KS statistical values versus redshift for three different probability functions of DM_{cosmic} .